

Two interacting electrons in a spherical box: An exact diagonalization study

David C. Thompson* and Ali Alavi

University of Cambridge, Chemistry Department, Lensfield Road, Cambridge CB2 1EW, United Kingdom

(Received 24 June 2002; Revised manuscript received 18 September 2002; published 31 December 2002)

We study a system of two electrons interacting with a Coulomb potential in a sphere of radius R , bounded by an infinite wall using exact diagonalization. We have also investigated the influence of an additional parabolic potential (of strength k) arising from a uniform background smeared throughout the sphere. The convergence of the ground state energy of the singlet spin state of the system is investigated as a function of sphere size (essentially r_s , the Wigner–Seitz density parameter) for cases where there is no background potential ($k=0$) and for when $k \neq 0$. With $k=0$ and small r_s , we observe a maximum in the ground state density at the origin of the sphere. At $r_s \approx 8$ a.u., the ground state density acquires a minimum at the origin. For this and larger systems we identify the formation of a “Wigner” molecule state. We further investigate the ground state density as a function of k and also the correlation hole density as a function of r_s and k . We invert the Kohn–Sham equation for a two electron system and calculate the local effective potential and correlation potential (to within an additive constant) as functions of the radial coordinate for a number of values of r_s and k .

DOI: 10.1103/PhysRevB.66.235118

PACS number(s): 71.15.Mb, 73.21.–b

I. INTRODUCTION

Improvements in experimental methods of confining electrons and in the techniques used to investigate these systems have been a rich source for theoretical investigation. Previous work employed a variety of confining potentials: spherical potential wells,¹ isotropic harmonic oscillator,² planar polygonal,³ and the infinite cuboidal⁴ and ellipsoidal⁵ confining geometries. In this paper we study the simple system of two interacting electrons confined to a spherical volume of space by an infinite potential. We solve this problem in a quasixact way using exact diagonalization, which enables us to calculate essentially exact solutions for the ground and excited states.

The introduction of a uniform background charge density throughout the interior of the sphere results in the particles moving in an attractive parabolic potential, giving rise to a model closely related to the “Hooke’s law” helium atom. The strength of this background charge density shall be denoted k . The Hooke’s law system is an analytically solvable^{6,7} model (for a certain infinite set of discrete oscillator frequencies) which has been studied extensively.^{8,9} It has a central attractive center where the electron-nuclear Coulomb interaction is described by a harmonic potential. These types of systems have the attractive property that the correlation between the confined particles can be varied simply by increasing or decreasing the size of the system, r_s , where r_s is linked to the radius of the sphere through $r_s = R/2^{1/3}$. An additional parameter (the steepness of the parabolic potential k) is introduced in the case of a nonzero compensating uniform background charge density. The two parameters r_s and k can be varied smoothly to take the system from the dense (weakly correlated) to the dilute (strongly correlated) regime. This class of exactly solvable model, can be used to study without any approximations, the complex nature of the exchange–correlation hole. Such investigations can lead to improvements to functionals beyond the local density approximation (LDA).^{8–10}

We have organized this paper as follows. In Sec. II we formulate the model whilst in Sec. III we discuss the general method of solution. In Sec. IV we evaluate the Coulomb integrals in terms of the coupled one particle basis. In Sec. V we formalize the density and exchange–correlation hole densities for this system, and in Sec. VI we introduce a background potential into the model through the smearing of a uniform positive charge throughout the interior of the sphere. In Sec. VII we invert the Kohn–Sham equation to find the local effective and correlation potentials, to within an additive constant. In Sec. VIII we report results of several calculations including energies, wave functions, exact densities, exact correlation holes and the Kohn–Sham and correlation potentials, as functions of r_s and k . Section IX is the conclusion.

II. THE MODEL

One might proceed in the spirit of Kestner and Sinanoğlu⁶ and seek solutions to the Schrödinger equation in terms of the center-of-mass and relative coordinates. This method is successful in the Hooke’s law helium, due to the fact that two separate Schrödinger equations arise, one for the center-of-mass coordinates and one for the relative coordinates. However for the present problem, such an approach yields a coupled set of Schrödinger equations as the confining potential, being infinite at the boundary, induces an awkward constraint on the relative coordinates when the center-of-mass coordinates are off-center. Therefore, in this paper we have chosen to proceed by looking for solutions in terms of the one-particle functions of the infinite spherical-well problem. These have the form¹¹

$$\eta_{nlm}(\mathbf{r}) = N_{nl} j_l(\alpha_{nl} r) Y_{lm}(\theta, \phi) = \langle \mathbf{r} | nlm \rangle, \quad (1)$$

where

$$N_{nl} = \frac{2}{R^3} (j_{l+1}(k_{nl}))^{-1} \quad (2)$$

and

$$\alpha_{nl} = \frac{k_{nl}}{R}. \quad (3)$$

Here the $j_l(r)$ are the spherical Bessel functions of order l and the $Y_{lm}(\theta, \phi)$ are the spherical harmonics. The k_{nl} are simply the n th roots of the l th order spherical Bessel function and R is the radius of the confining sphere. Equation (3) ensures that the wavefunction vanishes at the boundary of the sphere.

The two-electron Hamiltonian for the problem (Hartree atomic units $\hbar = m_e = e^2 = 1$ are used throughout) becomes

$$\hat{H} = \hat{T} + \hat{U} + \hat{V}, \quad (4)$$

$$\hat{T} = -\frac{1}{2} \sum_{i=1}^2 \nabla_i^2, \quad (5)$$

$$\hat{U} = \frac{1}{|\mathbf{r}_1 - \mathbf{r}_2|}, \quad (6)$$

$$\hat{V} = \sum_{i=1}^2 v_{\text{ext}}(\mathbf{r}_i), \quad (7)$$

where we define the external potential to be

$$v_{\text{ext}}(\mathbf{r}) = \begin{cases} \frac{1}{2} k r^2, & r < R, \\ 0, & r \geq R. \end{cases} \quad (8)$$

This external potential can be thought of as arising through the introduction of a uniform compensating background charge, such that the value of k corresponding to an overall charge-neutral system is given by

$$k = \frac{2}{R^3}. \quad (9)$$

Our Hamiltonian contains two parameters and for $R = \infty$ and $k > 0$ we would recover the Hooke's law atom. With $k = 0$ and R finite we have an ideal confined electron problem. In both cases the "strongly" correlated limit can be achieved by letting R become large or k small.

III. METHOD OF SOLUTION

We define a two-body wave function $\Psi(\mathbf{x}_1, \mathbf{x}_2)$ which we decompose into a spatial wave function $\Psi^\pm(\mathbf{r}_1, \mathbf{r}_2)$ and a spin wave function $\chi^\mp(\sigma_1, \sigma_2)$:

$$\Psi(\mathbf{x}_1, \mathbf{x}_2) = \Psi^\pm(\mathbf{r}_1, \mathbf{r}_2) \chi^\mp(\sigma_1, \sigma_2). \quad (10)$$

We can then expand the spatial wave function as a linear

combination of symmetrized (or antisymmetrized) one particle solutions, which in ket notation becomes

$$\begin{aligned} \langle \mathbf{r}_1 \mathbf{r}_2 | n_1 l_1 m_1 n_2 l_2 m_2 \rangle = N_K [& \langle \mathbf{r}_1 | n_1 l_1 m_1 \rangle \langle \mathbf{r}_2 | n_2 l_2 m_2 \rangle \\ & \pm \langle \mathbf{r}_2 | n_1 l_1 m_1 \rangle \langle \mathbf{r}_1 | n_2 l_2 m_2 \rangle]. \end{aligned} \quad (11)$$

The N_K are chosen such as to normalize Eq. (11),

$$N_K = \frac{1}{\sqrt{2 + 2 \delta_{n_1 n_2} \delta_{l_1 l_2} \delta_{m_1 m_2}}}. \quad (12)$$

Due to the spherical symmetry of the system it is most efficient to work in a coupled representation such that we can expand these coupled basis functions in terms of the uncoupled, one particle functions, such that

$$\begin{aligned} |n_1 l_1 n_2 l_2 LM\rangle = \sum_{m_1 m_2} |n_1 l_1 m_1 n_2 l_2 m_2\rangle \\ \times \langle n_1 l_1 m_1 n_2 l_2 m_2 | n_1 l_1 n_2 l_2 LM \rangle \end{aligned} \quad (13)$$

with $\langle n_1 l_1 m_1 n_2 l_2 m_2 | n_1 l_1 n_2 l_2 LM \rangle$, by definition, the $3j$ -Wigner symbols. L must satisfy the triangular inequality,¹²

$$l_1 + l_2 \geq L \geq |l_1 - l_2|, \quad (14)$$

and M is constrained to be

$$M = m_1 + m_2. \quad (15)$$

L and M are constants of the motion and uniquely define any given spatial wave function $\Psi_{LM}^\pm(\mathbf{r}_1, \mathbf{r}_2)$.

To further simplify notation we define

$$\mathbf{G} = \{n_1 l_1 n_2 l_2\}, \quad (16)$$

a four-dimensional vector of quantum numbers. We can now express $\Psi_{LM}^\pm(\mathbf{r}_1, \mathbf{r}_2)$ as

$$\Psi_{LM}^\pm(\mathbf{r}_1, \mathbf{r}_2) = \sum_{\mathbf{G}} c_{\mathbf{G}}^\pm |n_1 l_1 n_2 l_2 LM\rangle = \sum_{\mathbf{G}} c_{\mathbf{G}}^\pm \Phi_{\mathbf{G}LM}^\pm. \quad (17)$$

The $c_{\mathbf{G}}^\pm$ are coefficients to be determined, and the sum over \mathbf{G} runs over all possible combinations of $\{n_1 l_1 n_2 l_2\}$, where $n_{1,2}$ and $l_{1,2}$ can have the maximum values n_{max} and l_{max} , respectively. The $\Phi_{\mathbf{G}LM}^\pm$ form a complete symmetric (or antisymmetric) set of basis functions that satisfies the boundary condition of the wave function being identically zero at the boundary of the sphere.

In the chosen basis the kinetic energy is diagonal, with matrix elements being of the form

$$\begin{aligned} \langle \Phi_{\mathbf{G}LM} | \hat{T} | \Phi_{\mathbf{G}'LM} \rangle &= \frac{1}{2} (\alpha_{n_1 l_1}^2 + \alpha_{n_2 l_2}^2) \delta_{\mathbf{G}\mathbf{G}'} \\ &= \frac{1}{2R^2} (k_{n_1 l_1}^2 + k_{n_2 l_2}^2) \delta_{\mathbf{G}\mathbf{G}'}. \end{aligned} \quad (18)$$

However, the Coulomb matrix elements in the required basis require a little more work and will be discussed in the next section. For the moment we will assume that they can be calculated accurately and efficiently.

The Schrödinger equation,

$$\hat{H}\Psi^\pm = E\Psi^\pm, \quad (19)$$

can now be rewritten as an eigenvalue equation in the unknown c_G^\pm such that for a given LM state:

$$\sum_{G'} \hat{H}_{GG'} c_{G'}^\pm = E^\pm c_G^\pm. \quad (20)$$

This is, so far, formally exact and if calculated as written the Ψ^\pm would be the exact wave functions to the problem, including the excited states. Of course, in practice, the finite number of basis functions Φ_{GLM}^\pm that can be practicably included prevent this from being an exact solution to the problem.

IV. COULOMB INTEGRALS

In order to evaluate the matrix elements of the Hamiltonian we need to be able to calculate the Coulomb matrix elements, and in doing so we need to be able to calculate integrals of the form

$$(n_1 l_1 m_1 n_2 l_2 m_2 | n'_1 l'_1 m'_1 n'_2 l'_2 m'_2) = \int \int \frac{\eta_{n_1 l_1 m_1}^*(\mathbf{r}_1) \eta_{n_2 l_2 m_2}^*(\mathbf{r}_2) \eta_{n'_1 l'_1 m'_1}(\mathbf{r}_1) \eta_{n'_2 l'_2 m'_2}(\mathbf{r}_2)}{|\mathbf{r}_1 - \mathbf{r}_2|} d\mathbf{r}_1 d\mathbf{r}_2. \quad (21)$$

In considering the Coulomb integrals for the symmetrized and antisymmetrized basis functions we find we have to consider the sum and difference of the direct $(n_1 l_1 m_1 n_2 l_2 m_2 | n'_1 l'_1 m'_1 n'_2 l'_2 m'_2)$ and exchange $(n_1 l_1 m_1 n_2 l_2 m_2 | n'_2 l'_2 m'_2 n'_1 l'_1 m'_1)$ integrals, which in terms of the coupled representation becomes

$$\langle \Phi_{GLM}^\pm | \hat{U} | \Phi_{G'L'M'}^\pm \rangle = 2N_K N_{K'} [(n_1 l_1 n_2 l_2 LM | n'_1 l'_1 n'_2 l'_2 L' M') \pm (n_1 l_1 n_2 l_2 LM | n'_2 l'_2 n'_1 l'_1 L' M')], \quad (22)$$

with the N_K being given by Eq. (12). The integrals appearing on the right-hand side of Eq. (22) are well known¹³ and in terms of the coupled representation become

$$\langle n_1 l_1 n_2 l_2 LM | \hat{U} | n'_1 l'_1 n'_2 l'_2 L' M' \rangle = \delta_{LL'} \delta_{MM'} \sum_k f_k(l_1 l_2 l'_1 l'_2; L) [R^{(k)}(n_1 l_1 n_2 l_2 n'_1 l'_1 n'_2 l'_2) + R^{(k)}(n_2 l_2 n_1 l_1 n'_2 l'_2 n'_1 l'_1)], \quad (23)$$

where

$$f_k(l_1 l_2 l'_1 l'_2; L) = \delta_{L'L} (-1)^{L+k} [(2l_1+1)(2l'_1+1)(2l_2+1)(2l'_2+1)]^{1/2} W(l_1 l_2 l'_1 l'_2; kL) \begin{pmatrix} k & l_1 & l'_1 \\ 0 & 0 & 0 \end{pmatrix} \begin{pmatrix} k & l_2 & l'_2 \\ 0 & 0 & 0 \end{pmatrix}. \quad (24)$$

Here $W(l_1 l_2 l'_1 l'_2; kL)$ is a Racah function and there are a number of restrictions placed on the allowed nonzero values of such a function. In Eq. (24) the $3j$ -Wigner symbols impose the restriction that $k+l_1+l'_1$ and $k+l_2+l'_2$ be even. Physically this is such that the $1/r_{12}$ interaction does not couple states of a different total parity. From these terms there is also the condition that $k \leq l_1+l'_1$ and $k \leq l_2+l'_2$. The $R^{(k)}$ are simply finite forms of the Slater radial integrals

$$R^{(k)}(n_1 l_1 n_2 l_2 n'_1 l'_1 n'_2 l'_2) = \int_{r_1=0}^R r_1^2 dr_1 \int_{r_2=0}^{r_1} r_2^2 dr_2 \frac{r_2^k}{r_1^{k+1}} N_{n_1 l_1 j_{l_1}}(\alpha_{n_1 l_1} r_1) N_{n'_1 l'_1 j_{l'_1}}(\alpha_{n'_1 l'_1} r_1) N_{n_2 l_2 j_{l_2}}(\alpha_{n_2 l_2} r_2) N_{n'_2 l'_2 j_{l'_2}}(\alpha_{n'_2 l'_2} r_2). \quad (25)$$

In calculating these Slater radial integrals the inner integral, formally a function of the radial variable r_1 , is calculated using a Gauss–Chebyshev routine¹⁴ over a mesh of 64 points. Tests were performed to ensure that convergence of the integrals with respect to mesh size had occurred over a range of sphere sizes and quantum numbers. This tabulation, a process which happens as an initialization step in the code, is done once in order to decrease computer time.

It was noticed that a whole class of Coulomb matrix elements could be solved analytically. These particular elements

have the form corresponding to each particle having zero total angular momentum. A closed form solution to them corresponds to solving the Slater radial integrals $R^{(0)}(n_1 0 n_2 0 n'_1 0 n'_2 0)$ for any combination of the radial quantum numbers. These analytic solutions provided an invaluable check when writing code, and they give us an idea of how accurate our numerical evaluation of these highly oscillatory radial integrals is. Table I shows some examples of the differences between the Coulomb matrix elements evaluated analytically and numerically, with the differences being extremely small. We note excellent agreement with the

TABLE I. Comparison of the numerical and analytic values of a selection of the Coulomb matrix elements with zero total angular momentum.

Element	Analytic	Numerical
$\langle 100100 \hat{U} 100100\rangle$	1.786073181	1.786073070
$\langle 100100 \hat{U} 200400\rangle$	0.00713410171	0.00713410153
$\langle 100200 \hat{U} 300400\rangle$	0.143623626	0.143623628
$\langle 200400 \hat{U} 300300\rangle$	0.621169740	0.621169745
$\langle 200300 \hat{U} 400400\rangle$	0.0583870328	0.0583870309

ground state $(100100|100100)$, Coulomb integral as calculated in Ref. 5.

V. ELECTRON DENSITY AND EXCHANGE-CORRELATION HOLE

One of the most interesting and potentially useful properties of these two-electron model systems, is that the density functional theory (DFT) when applied to them can be greatly simplified. We know that for any two-electron system we can write

$$n(\mathbf{r}_1) = 2 \int |\Psi_{LM}^{\pm}(\mathbf{r}_1, \mathbf{r}_2)|^2 d\mathbf{r}_2. \quad (26)$$

Substituting the form of the two-body wave function given previously into Eq. (26) results in

$$n(\mathbf{r}_1) = 2 \sum_{GG'} c_G^{\pm} c_{G'}^{\pm} S_{GG'}, \quad (27)$$

with the c_G the wave function coefficients and

$$S_{GG'} = \int \Phi_{GLM}^{\pm*} \Phi_{G'LM}^{\pm} d\mathbf{r}_2. \quad (28)$$

The density is a scalar quantity and is thus independent of choice of axes, it is also independent of rotations about the chosen axes. Given this, we are able to integrate out the angular dependence in Eq. (26). Formally we integrate Eq. (27) with respect to the solid angle Ω_1 , such that

$$n(r_1) = \int n(\mathbf{r}_1) d\Omega_1 = \frac{1}{2\pi} \sum_{GG'} c_G c_{G'} \int S_{GG'} d\Omega_1. \quad (29)$$

Computationally, the evaluation of the density for this model is the quickest part of the whole calculation. Having a density that is extremely easy to calculate is an attractive feature of this system, as all properties of the system can be derived from the density.

The physical exchange-correlation hole is defined in DFT in terms of the density-density correlation function evaluated with the two-body wave function, given by Eq. (17), such that

$$n_{xc}(\mathbf{r}_1, \mathbf{r}_2) = \frac{1}{n(\mathbf{r}_1)} \langle \Psi | \delta \hat{n}(\mathbf{r}_1) \delta \hat{n}(\mathbf{r}_2) | \Psi \rangle - \delta(\mathbf{r}_1 - \mathbf{r}_2), \quad (30)$$

where

$$\delta \hat{n}(\mathbf{r}) = \hat{n}(\mathbf{r}) - n(\mathbf{r}), \quad (31)$$

and $\hat{n}(\mathbf{r})$ is the number density operator

$$\hat{n}(\mathbf{r}) = \sum_i \delta(\mathbf{r} - \mathbf{r}_i). \quad (32)$$

In the preceding expressions, subscripts and superscripts have been omitted for clarity. These general expressions can be greatly simplified for this two electron system and we find that the exchange-correlation hole given by Eq. (30) can be written solely in terms of the density and the two-body wave function

$$n_{xc}(\mathbf{r}_1, \mathbf{r}_2) = \frac{2|\Psi(\mathbf{r}_1, \mathbf{r}_2)|^2}{n(\mathbf{r}_1)} - n(\mathbf{r}_2). \quad (33)$$

This quantity is normalized to -1 .

The correlation hole density $n_c(\mathbf{r}_1, \mathbf{r}_2)$ can be calculated by subtracting off the exchange hole density $n_x(\mathbf{r}_1, \mathbf{r}_2)$, which for any two-electron system is given by

$$n_x(\mathbf{r}_1, \mathbf{r}_2) = -\frac{n(\mathbf{r}_2)}{2}. \quad (34)$$

Therefore we find

$$n_c(\mathbf{r}_1, \mathbf{r}_2) = \frac{2|\Psi(\mathbf{r}_1, \mathbf{r}_2)|^2}{n(\mathbf{r}_1)} - \frac{n(\mathbf{r}_2)}{2}, \quad (35)$$

where the correlation hole density is normalized to zero. This expression has a useful qualitative interpretation: $|\Psi(\mathbf{r}_1, \mathbf{r}_2)|^2$ is the probability of finding one electron at \mathbf{r}_1 and another at \mathbf{r}_2 . Dividing this by the probability of finding an electron at \mathbf{r}_1 , yields a conditional probability of finding an electron at \mathbf{r}_2 given that the other is at \mathbf{r}_1 . If this conditional probability is larger than the probability of finding an electron at \mathbf{r}_2 , then $n_c(\mathbf{r}_1, \mathbf{r}_2)$ is positive, otherwise it is negative. When would we expect these two situations to occur? If \mathbf{r}_2 is chosen close to the reference point \mathbf{r}_1 , the chances of finding another electron at \mathbf{r}_2 given there is already an electron at \mathbf{r}_1 , is small and therefore in the vicinity of \mathbf{r}_1 the correlation hole will be negative. Conversely, if \mathbf{r}_2 is chosen to be a large distance from \mathbf{r}_1 , then the probability of finding another electron at \mathbf{r}_2 might be larger than expected (due to correlation) and thus $n_c(\mathbf{r}_1, \mathbf{r}_2)$ may be positive. Electron correlation is responsible for the positive regions of the exchange-correlation hole. An investigation of the oscillations in the sign of $n_c(\mathbf{r}_1, \mathbf{r}_2)$ will enable us to understand, at least qualitatively, the spatial correlation between the electrons in any given state. As an example, if the electrons are seen to localize in well defined regions of space (as would be the case upon formation of a Wigner molecule) we would expect the correlation hole, and the exchange-correlation

hole, to be strongly positive at some value of separation. On the other hand, if the electrons are uncorrelated throughout space the correlation hole will not be strongly positive and the exchange–correlation hole will be predominantly negative.

Although formally the correlation hole is a six-dimensional function, the spherical symmetry of the problem reduces the dimensionality to three so that Eq. (35) can be written simply as

$$n_c(r_1, r_2, \theta) = \frac{2|\Psi(r_1, r_2, \theta)|^2}{n(r_1)} - \frac{n(r_2)}{2}. \quad (36)$$

This functional form allows us to fix r_1 and vary either r_2 or θ .

VI. A UNIFORM BACKGROUND POTENTIAL

Overall charge neutrality is imposed upon the system by smearing a positive uniform background charge throughout

the interior of the sphere. This is done by allowing a background charge density, $\rho(\mathbf{r})$, to take the form

$$\rho(\mathbf{r}) = \begin{cases} k\rho, & r < R, \\ 0, & r \geq R \end{cases} \quad (37)$$

with

$$\rho = \frac{2}{\Omega}. \quad (38)$$

Ω is simply the volume of the enclosing sphere and k should be identified with the harmonic potential prefactor as defined by Eq. (8).

In order to diagonalize the Hamiltonian, matrix elements of the form $\langle \Phi_{\mathbf{G}} | \hat{V} | \Phi_{\mathbf{G}'} \rangle$ have to be evaluated. These elements have the form

$$\begin{aligned} \langle \Phi_{\mathbf{G}LM}^\pm | \hat{V} | \Phi_{\mathbf{G}'LM}^\pm \rangle = & \frac{1}{2} k \left[\delta_{\mathbf{n}_2 \mathbf{n}_2'} \delta_{l_1 l_1'} \delta_{m_1 m_1'} \int_0^R N_{n_1 l_1} j_{l_1}(\alpha_{n_1 l_1} r_1) N_{n_1' l_1'} j_{l_1'}(\alpha_{n_1' l_1'} r_1) r_1^4 dr_1 \right. \\ & \left. + \delta_{\mathbf{n}_1 \mathbf{n}_1'} \delta_{l_2 l_2'} \delta_{m_2 m_2'} \int_0^R N_{n_2 l_2} j_{l_2}(\alpha_{n_2 l_2} r_2) N_{n_2' l_2'} j_{l_2'}(\alpha_{n_2' l_2'} r_2) r_2^4 dr_2 \right], \end{aligned} \quad (39)$$

where for compactness, we introduce the notation

$$\mathbf{n} = (nlm). \quad (40)$$

These one dimensional integrals are evaluated quickly and accurately using a Gauss–Chebyshev integration routine.¹⁴ The introduction of a uniform background charge provides another variable parameter with which to probe the correlation of the system.

VII. THE KOHN–SHAM AND CORRELATION POTENTIALS

Another interesting property of this, and indeed any two electron system, is that we can directly relate the density to the one electron Kohn–Sham orbitals such that for two electrons of opposite spin the Kohn–Sham orbital is simply related to the electronic density via

$$n(\mathbf{r}) = 2\phi^2(\mathbf{r}). \quad (41)$$

The Kohn–Sham orbital, $\phi(\mathbf{r})$, and corresponding eigenvalue, ϵ , satisfy the Kohn–Sham equation which describes the noninteracting system

$$\left[-\frac{1}{2}\nabla^2 + v_{\text{eff}}(\mathbf{r}) \right] \phi(\mathbf{r}) = \epsilon \phi(\mathbf{r}). \quad (42)$$

We can readily invert Eq. (42) in order to find $v_{\text{eff}}(\mathbf{r})$ to within an additive constant—the Kohn–Sham eigenvalue,

$$v_{\text{eff}}(\mathbf{r}) = \epsilon + \frac{1}{2} \frac{\nabla^2 n^{\frac{1}{2}}(\mathbf{r})}{n^{\frac{1}{2}}(\mathbf{r})}. \quad (43)$$

A knowledge of the exact ground state density, $n(\mathbf{r})$, from a correlated wave function therefore enables one to compute $v_{\text{eff}}(\mathbf{r}) - \epsilon$. Furthermore, we can write

$$v_{\text{eff}}(\mathbf{r}) = v_{\text{ext}}(\mathbf{r}) + v_x(\mathbf{r}) + v_c(\mathbf{r}) + v_{\text{Hart}}(\mathbf{r}), \quad (44)$$

where v_x and v_c are the separate exchange and correlation potentials. Since,

$$v_x(\mathbf{r}) = \frac{\delta E_x}{\delta n(\mathbf{r})}, \quad (45)$$

with

$$E_x = \frac{1}{2} \int \frac{n(\mathbf{r})n_x(\mathbf{r}, \mathbf{r}')}{|\mathbf{r} - \mathbf{r}'|} d\mathbf{r} d\mathbf{r}', \quad (46)$$

for two electron systems we can use Eq. (34) to relate the exact exchange potential to the Hartree potential

$$v_x(\mathbf{r}) = -\frac{1}{2} v_{\text{Hart}}(\mathbf{r}). \quad (47)$$

Using these relationships we find that we can compute the correlation potential (from the exact electron density) to within an additive constant

TABLE II. Energy convergence as a function of sphere size, for $k=0$.

Radius of sphere	r_s /a.u.	n, l	No. of basis functions	Energy/a.u.	Relative error
1	0.79	1,1	3	11.643018677	0.169%
		2,2	21	11.624207716	0.007%
		3,3	78	11.623559564	0.0017%
		4,3	136	11.623487792	0.0012%
		4,4	210	11.623430654	0.0006%
			∞	11.62335(2)	
5	3.97	1,1		0.739147316	2.13%
		2,2		0.724069582	0.05%
		3,3		0.723786342	0.011%
		4,3		0.723764057	0.0078%
		4,4		0.723740152	0.0045%
			∞	0.723707(3)	
20	15.87	1,1		0.103409312	8.35%
		2,2		0.095697381	0.273%
		3,3		0.095445451	0.010%
		4,3		0.095438065	0.002%
		4,4		0.095437266	0.001%
			∞	0.0954361(8)	

$$v_c(\mathbf{r}) - \epsilon = \frac{1}{2} \frac{\nabla^2 n^{\frac{1}{2}}(\mathbf{r})}{n^{\frac{1}{2}}(\mathbf{r})} - \frac{1}{2} v_{\text{Hart}}(\mathbf{r}) - v_{\text{ext}}(\mathbf{r}). \quad (48)$$

Expressed in this form, the correlation potential has a kinetic contribution and a self-interaction correction term, which in the present case is simply $-\frac{1}{2}v_{\text{Hart}}(\mathbf{r})$.

VIII. RESULTS

We shall be studying a confining sphere of radius R , and will only be concerned with the ground state of the system (i.e., the $L=0, M=0$ state). We denote n_{max} and l_{max} to be the largest wave numbers allowed in the basis of η 's [Eq. (1)]. For any given n_{max} and l_{max} , the Hamiltonian was diagonalized using a direct diagonalization method.¹⁵ We have investigated the form of the wave function, density, correlation hole, Kohn–Sham and correlation potentials for a range of r_s and for different values of k in the case of the uniform background study.

A. Convergence with n_{max} and l_{max}

We first examine the convergence of the total energy of the system with increasing n_{max} and l_{max} as a function of r_s . We consider n_{max} from 1 to 4 and l_{max} from 0 to 4. Table II shows total energies for a number of r_s for the singlet $L=0, M=0$ wave function for the case $k=0$, i.e., in the absence of a uniform background charge. We see that the energy decreases on increasing both of n_{max} and l_{max} , this is of course, due to the energy being variational with respect to both of these parameters. We define the relative error in the

TABLE III. Energy convergence for the charge-neutral unit sphere.

Radius of sphere	r_s /a.u.	n, l	No. of basis functions	Energy/a.u.	Relative error
1	0.79	1,1	3	12.208587646	0.091%
		2,2	21	12.198445438	0.007%
		3,3	78	12.197755765	0.002%
		4,3	136	12.197679819	0.0011%
		4,4	210	12.197623086	0.0006%
			∞	12.19754(5)	

energy with respect to the infinite basis energy limit (calculated in the manner of Halkier *et al.*¹⁶). Upon increasing r_s we observe a slower convergence, as measured by the relative error. We expect that for $k \neq 0$, the effect of the uniform background potential (which is to be thought of as a parabolic well) would be to push the electrons into the center of the sphere, thus increasing the energy of the system. Table III shows that this is indeed the case.

B. The ground state wave function

It is interesting to observe how the wave functions evolve as a function of r_s . We concentrate on the overall ground state $L=0, M=0$ with $k=0$. The absolute values of the wave function coefficients are shown in Fig. 1. As r_s increases we observe a decrease in the contribution from the $|100100\rangle$ state along with an increase in the contributions from higher states (e.g., $|100200\rangle$, $|110110\rangle$, and $|200200\rangle$). It is instructive to understand this change in terms of the one particle states $|nlm\rangle$ of Eq. (1). The energies associated with these one particle solutions are simply

$$E_{nl} = \frac{\alpha_{nl}^2}{2R^2} \quad (49)$$

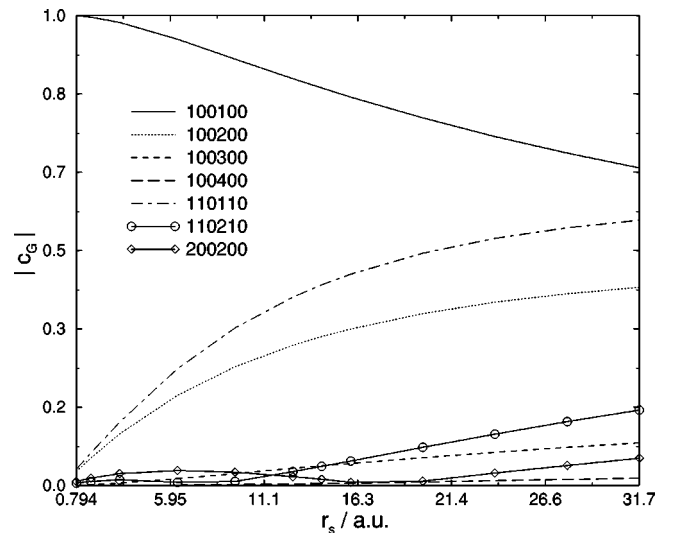


FIG. 1. Absolute value of wave function coefficients for singlet, $L=0, M=0$ ground state as a function of r_s , here $n_{\text{max}}=4, l_{\text{max}}=4$, and $k=0$.

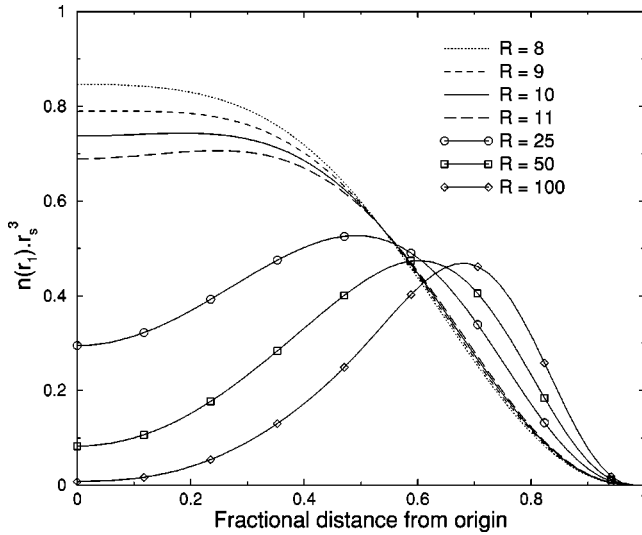


FIG. 2. Ground state ($L=0, M=0$) electron density as a function of R for $k=0$. The density is seen to form a minimum at the origin of the sphere for $r_s \approx 8$. The formation of a minimum is indicative of the system moving into a Wigner molecule phase where correlation between the particles is the dominant factor. The horizontal axis is the fractional distance from the origin. To enable comparisons between systems of differing size, we have normalized distances to that of the unit sphere. This convention is adopted throughout.

for any given n and l . The influence of the confining potential causes striking differences from a hydrogenic energy level scheme. In the hydrogenic Schrödinger equation a centrifugal term, $\hbar^2[l(l+1)/r^2]$ ensures that a given state specified by the principle quantum number, n , can only have certain angular momentum states. In the present model, because of the infinite confining potential, this accidental degeneracy between the n and l states is broken. Subsequently there is an n quantum number associated with each angular momentum separately.

We see that the spacing between any two levels goes as $\sim 1/R^2$, so as the confining sphere becomes larger the energy gap between successive levels becomes smaller, allowing population of higher angular momentum states. The true ground state for a high density system (small r_s) would be the population of the $1s$ state by both electrons. However for larger spheres, as the gap between energy levels decreases, it is energetically favorable for an electron to be in a higher angular momentum state thus reducing electron–electron repulsion occurring from double occupation of the same orbital.

C. The ground state density

The singlet ground state density (for $k=0$) is shown in Fig. 2 for a range of values of R . We see that for an $r_s < 8$ a.u., the density has a maximum at the origin of the sphere. For $r_s \approx 8$ a.u., the density acquires a minimum at the origin, which becomes more pronounced as R increases. At the same time the maximum in the density progresses towards the boundary of the sphere. This development of a

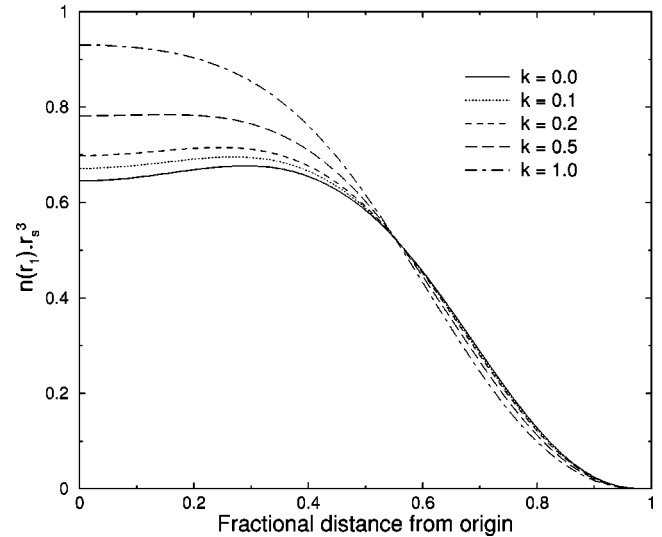


FIG. 3. Ground state ($L=0, M=0$) electronic density as a function of k for $R=12$. A small increase in the strength of the confining potential is seen to remove the minimum at the origin.

minimum is indicative of the formation of a “Wigner” molecule; in varying R we move from a strongly uncorrelated system (small R) where kinetic energy dominates to a strongly correlated regime (large R) where the electrostatic interaction is dominant. As R increases the correlation between the particles becomes paramount.

It is also interesting to compare this work with a related study of electrons confined to a hard walled cube⁴ where we find approximately the same value of r_s for formation of the Wigner molecule. This is somewhat unsurprising as the density at the origin is going to be insensitive to the confining potential for systems large enough to form a Wigner molecule. However, we would expect that a detailed analysis of other properties, for example, $n_c(r_1, r_2, \theta)$, near the confining boundary would yield results that were strongly potential dependent.

We also examine the form of the density for $k \neq 0$. In Fig. 3 we consider (for a number of different values of k) the example of a system for which we are just inside the regime of forming the Wigner molecule. We see that it requires a relatively small value of k to remove the minimum in the density at the origin and to move back into an “uncorrelated” phase. A nonzero value of k means that the electrons are moving in a potential which pushes them towards the center of the sphere. As k increases in magnitude the potential for the electrons to be at the origin of the sphere is competing with the tendency of the electrons to be as far apart as possible.

When $k=1$, the system is charge-neutral and in Fig. 4 we see a number of densities for a variety of different sized spheres. We observe that in this system there is a characteristic value of R at which we develop a minimum at the origin, thus recovering the Wigner molecule. For $R \approx 17$ we observe formation of a minimum at the origin, corresponding to $r_s \approx 13$ a.u. However, the qualitative behavior of the density does not change.

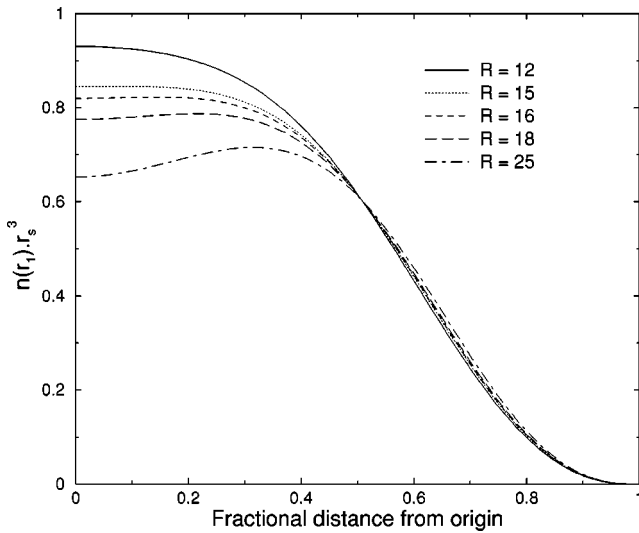


FIG. 4. Ground state ($L=0$, $M=0$) electronic density as a function of R for the charge-neutral system $k=1$. We find that for $r_s \approx 13$ a.u. we recover the Wigner molecule state.

D. The ground state correlation hole

Figure 5 shows $n_c(r_1, r_2, \theta)$ for $k=0$, $r_1=0$ and $\theta=\pi$ for several values of R . Although we explicitly define θ , with r_1 at the origin there is no θ dependence and the correlation hole density is a function of the radial coordinate r_2 . For small R , where we are in an uncorrelated system, the correlation hole is predominately negative. From our qualitative analysis of the form of the correlation hole given in Sec. V we see that this corresponds to low levels of spatial correlation, as we would expect from a system of a size such that the kinetic energy is the dominant term. Upon increasing R , we see from Fig. 2, that the density acquires a maximum and this maximum is seen to move to the boundary of the sphere. This is indicative of the increased importance of the Coulombic energy terms and consequently the correlation hole be-

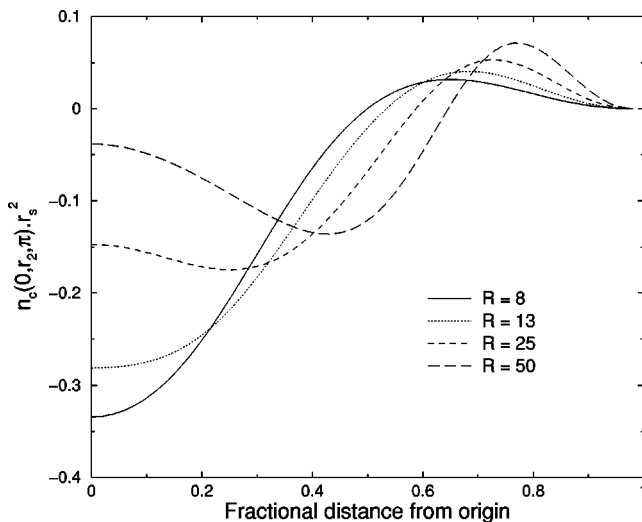


FIG. 5. Ground state ($L=0$, $M=0$) correlation hole as a function of R . Observe the enhancement of the correlation hole at the origin for large sphere sizes.

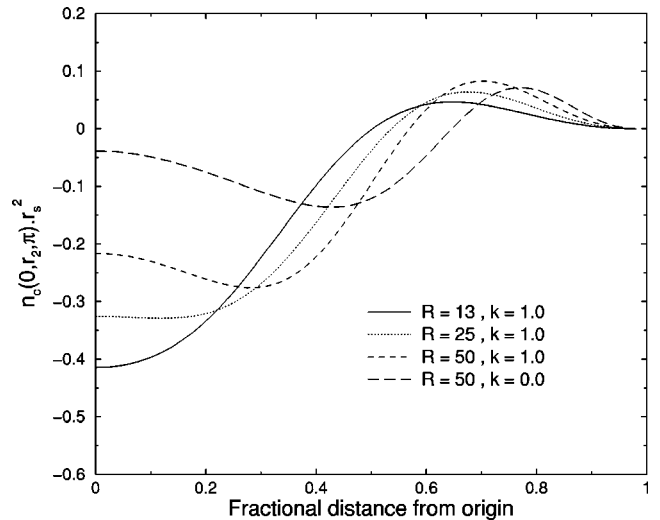


FIG. 6. Ground state ($L=0$, $M=0$) correlation hole as a function of R for charge-neutral systems. The long-dashed plot is a system with no background charge density to be used for comparison.

comes positive; there is an enhanced probability of finding the “other” electron away from the reference electron which is fixed at the origin. Interestingly, as $n(r)$ develops a minimum, i.e., on moving into the Wigner molecule, we develop a local maximum around the origin in the correlation hole. This becomes more pronounced the larger the sphere becomes, corresponding to regions of space where the electron is more likely to be with respect to the other. This spatial anisotropy in the correlation hole density is a counterintuitive result, although it should be remembered that in comparing these regions around the reference particle we are still concerned with correlation hole densities that are negative.

We see in Fig. 6 the variation of $n_c(r_1, r_2, \theta)$ for a number of R with $r_1=0$, $\theta=\pi$, and $k=1$ (the case of a charge-neutral sphere). For $k \neq 0$ the correlation hole for large spheres remains negative throughout space, with no local maximum in the origin. We find that for large enough spheres we can recover this maximum and all of the results concur with observations made in our discussion of Fig. 5.

In Figs. 7 and 8 we show contour plots for the singlet, ground state correlation hole. In all of these plots $R=15$, $r_s=11.91$ a.u. and in the absence of a background charge density ($k=0$) we can assume that we are inside the Wigner molecule regime. The darker regions in Figs. 7 and 8 correspond to areas where $n_c(r_1, r_2, \theta) < 0$, while the lighter areas have $n_c(r_1, r_2, \theta) > 0$. In Figs. 7(a, b) the reference electron is fixed at the origin and in Figs. 8(a, b) it is slightly displaced from the origin. In Fig. 7(a), with $k=0$, there is a region of space where the correlation hole is positive, as observed in Figs. 5 and 6. The well defined regions of positive and negative correlation imply a strong degree of localization and is indicative of the formation of a Wigner molecule. In the presence of a compensating background charge density, Fig. 7(b), the correlation hole becomes more negative around the origin. This contraction is caused by the additional attractive potential and diminishes the spatial correlation between the particles. In Fig. 8 upon displacing the

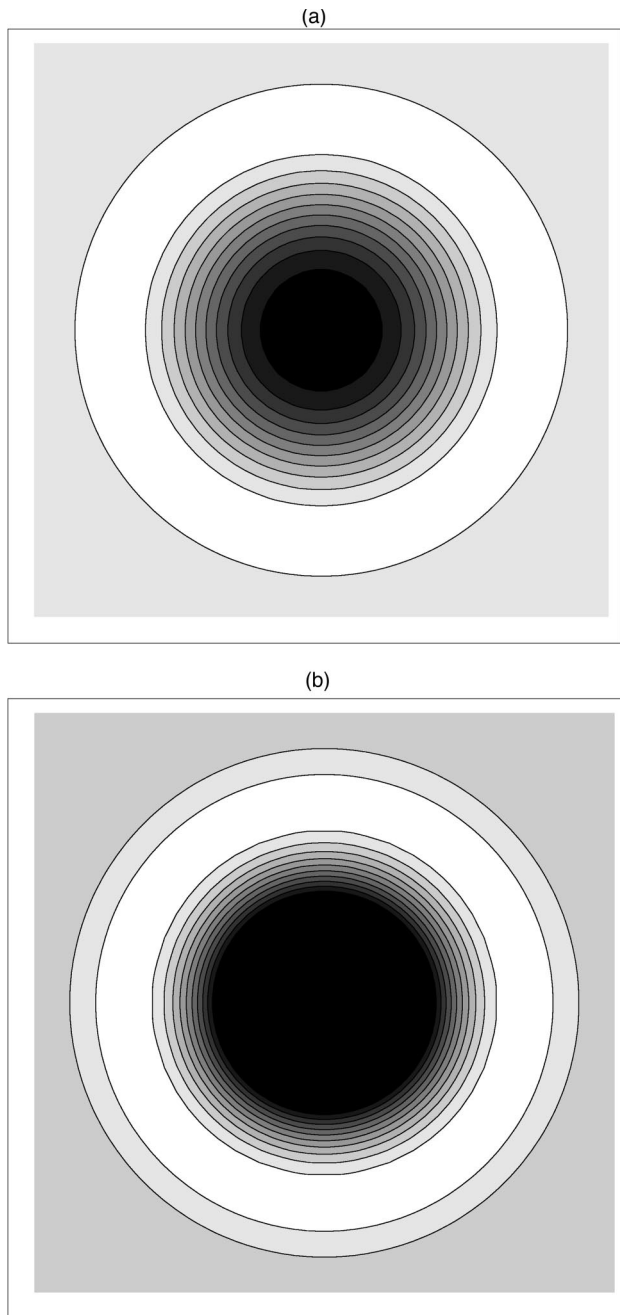


FIG. 7. Ground state ($L=0$, $M=0$) correlation hole contour plots for the $R=15$, $r_1=0$, $k=0$ (a) and charge-neutral systems, $k=1$ (b). Areas of dark shading represent negative regions of the correlation hole, while regions with lighter shading are to be associated with positive values of the correlation hole. For the $k=1$ case, (b), we see that the correlation hole is deeper (contracted) around the reference particle which is positioned at the origin of the sphere.

reference particle from the origin ($r_1=0.1R$), we see that the correlation hole is now theta dependent. Once again, the effect of the compensating background charge density is seen, in Fig. 8(b), to cause a contraction of the correlation hole around the reference particle.

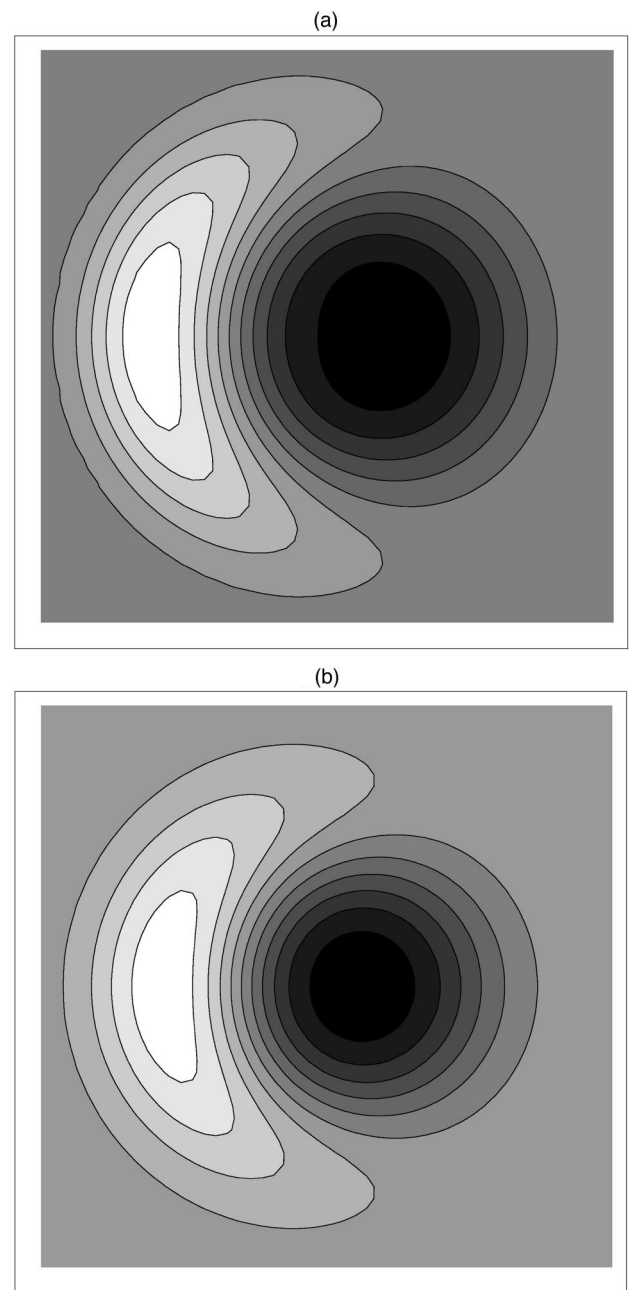


FIG. 8. Ground state ($L=0$, $M=0$) correlation hole contour plots for the $R=15$, $r_1=0.1R$, $k=0$ (a) and charge-neutral systems, $k=1$ (b). Areas of dark shading represent negative regions of the correlation hole, while regions with lighter shading are to be associated with positive values of the correlation hole. Here we observe strong directional correlation between particles and a contraction around the reference particle in the charge-neutral case.

E. The Kohn–Sham and correlation potentials

In Fig. 9 we present the Kohn–Sham effective potential for our two electron system arising from Eq. (43) for a number of different sphere sizes for $k=0$ and the charge-neutral system $k=1$. In both instances $v_{\text{eff}}(r) - \epsilon$ is plotted for sphere sizes just inside and outside the Wigner molecule regime. Since we are calculating the effective potential to

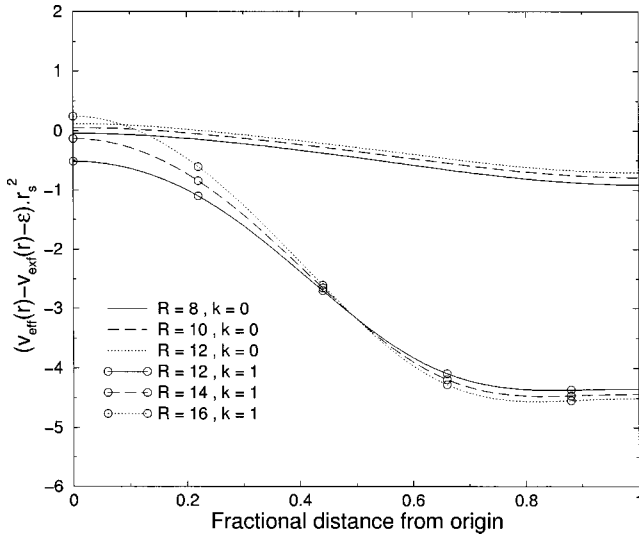


FIG. 9. The ground state ($L=0$, $M=0$) Kohn–Sham potential (to within an additive constant) as a function of r_s , for $k=0$ and $k=1$. We see that upon forming the Wigner molecule the potential becomes increasingly more repulsive at the origin. In the charge-neutral system we observe a flattening of the potential at large distances, due to the additional confining parabolic potential.

within an additive constant only the shape of the curve is important. We see that upon moving through the transition into the Wigner molecule the potential becomes increasingly repulsive at the origin, while becoming more attractive at the sphere boundary. We can relate the behavior of the potential at the origin to the changes in the exact ground state density for large R . An additional flattening of the potential at large distances from the origin is observed in the case of the charge-neutral system. In this instance the additional parabolic potential is seen to soften the effect of the infinite confining surface.

Figures 10(a, b) show the correlation potential $v_c(r) - \epsilon$, for high density [(a) $R=1$] and low density [(b) $R=20$] systems in the absence of a background potential ($k=0$). Also shown are the Hartree, effective and exchange potentials as defined in Sec. VII.

In the high density example there is no structure in the correlation potential, indicative of the dominating kinetic factors. We see in the low density system that the correlation potential has a clear maximum at the origin with a broad minimum upon moving away towards the sphere boundary, mirroring the form of the electronic density and the increasing dominance of the Coulomb interaction. In both systems the Hartree potential tends to a finite value at the sphere boundary. It is straightforward to show that for all systems confined by such a potential $v_{\text{Hart}}(R) \cdot r_s = 2^{2/3}$ and is thus independent of system size.

It is instructive to note the qualitative differences between the form of the correlation potential as presented in Fig. 10 and with those calculated in other model systems^{8–10} and in actual atomic systems (see, for example, Ref. 17).

As one of our long term objectives is to develop functionals beyond the generalized gradient approximation (GGA) we also compare the exact correlation potential to those gen-

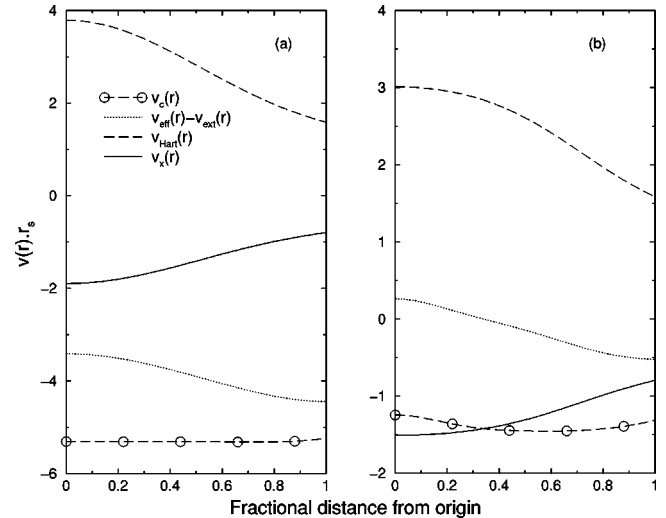


FIG. 10. A decomposition of the effective potential into contributions from the Hartree, exchange and correlation potentials. We consider the ground state ($L=0$, $M=0$) in the absence of a background potential ($k=0$) for $R=1$ (a) and $R=20$ (b). Note the change in scale from Fig. 9.

erated using the exact ground state density and commonly used functionals. We have used the Perdew–Zunger¹⁷ local density functional and the LYP,¹⁸ P91¹⁹ and PBE²⁰ GGA functionals. The subroutines used to generate the potentials are from the CADPAC²¹ computational suite. Results are shown in Fig. 11. None of the functionals are able to reproduce the exact potential. The Perdew–Zunger does remarkably well in reproducing the general shape as does the LYP

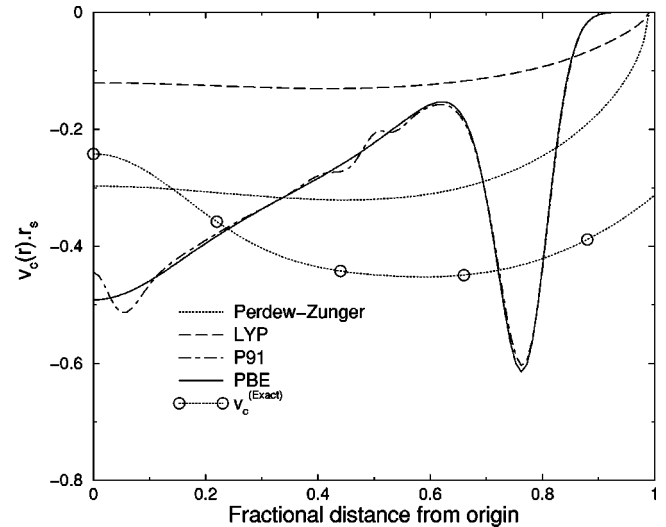


FIG. 11. A comparison of correlation potentials generated from commonly used functionals and the exact result generated in this study. The exact ground state density was used throughout for a system of size $R=20$. In order to compare the general shapes of the curves the exact potential has been rigidly shifted. We have used the LYP, P91, and PBE GGA functionals along with the Perdew–Zunger local functional. We see that none of the commonly used functionals are able to reproduce the shape of the exact curve. The LYP and PZ functionals do reasonably well at reproducing a maximum at the origin and a shallow minimum some distance from it.

GGA functional, based as it is upon the Colle–Salvetti²² functional which was in turn fitted to the helium atom. The GGA’s P91 and PBE exhibit a very deep minimum, which would tend to stabilize a Wigner molecule, but the overall shape of the potential is clearly unphysical. A similar failure for atomic helium has been noted by Umrigar *et al.*²³

IX. CONCLUSION

In this paper we have studied the quantum-mechanical behavior of two interacting electrons confined to a spherical volume of space by a hard infinite potential. We have also imposed an additional parabolic potential due to a uniform background charge which is smeared throughout the confining volume. We have used an exact diagonalization method, whereby we express the wave functions as linear combinations of symmetrized or antisymmetrized products of the one particle solutions. Due to the symmetry of the system we were able to introduce the quantum numbers L and M , which are constants of the motion, and represent the problem in a coupled representation. These two numbers precisely define any given wave function. We can calculate well converged energies for $n_{\max}=4$ and $l_{\max}=3$ for any given r_s .

With this technique we have studied the singlet ground state as a function of increasing R . A “Wigner” molecule

state is seen to form at large R and using the density and correlation hole we have been able to probe much of the rich physics of this system. We are further able to tune the system using the strength of the additional confining parabolic potential, k . Once inside the Wigner molecule phase we are able to “dissociate” this state through increasing the value of k . We see that in the charge-neutral system ($k=1$) there exists an R such that we can return to a strongly correlated (Wigner) state.

An exact solution of a model system such as this where the electron–electron interaction is a realistic one, and can be varied smoothly as a function of two free parameters, provides us with real insight into the correlation of two electron atomic systems. It would seem from our analysis of commonly used GGAs (Fig. 11) that there may be missing long range correlation interactions and a model such as ours provides an exact framework for investigating this and either moving beyond the GGA formalism, or improving existing functionals.

ACKNOWLEDGMENT

This work has been funded through an E.P.S.R.C. studentship. D.C.T. would like to thank Dr. A. J. Cohen for helpful discussions.

*Electronic address: dt236@cam.ac.uk

¹S. Bednarek, B. Szafran, and J. Adamowski, Phys. Rev. B **59**, 13 036 (1999).

²D. Pfannkuche, V. Gudmundsson, and P.A. Maksym, Phys. Rev. B **47**, 2244 (1993).

³C.E. Creffield, W. Häusler, J.H. Jefferson, and S. Sarker, Phys. Rev. B **59**, 10 719 (1999).

⁴A. Alavi, J. Chem. Phys. **113**, 7735 (2000).

⁵G. Cantele, D. Ninno, and G. Iadonisi, Phys. Rev. B **64**, 125325 (2001).

⁶N.R. Kestner and O. Sinanoğlu, Phys. Rev. **128**, 2687 (1962).

⁷M. Taut, Phys. Rev. A **48**, 3561 (1993).

⁸S. Kais, D.R. Herschbach, N.C. Handy, C.W. Murray, and G.J. Lamming, J. Chem. Phys. **99**, 417 (1993).

⁹P.M. Laufer and J.B. Krieger, Phys. Rev. A **33**, 1480 (1986).

¹⁰C. Filippi, C.J. Umrigar, and M. Taut, J. Chem. Phys. **100**, 1290 (1993).

¹¹E. Landau and E. Lifshitz, *Quantum Mechanics: Nonrelativistic Theory* (Addison-Wesley, Reading, MA, 1958).

¹²P. A. M. Dirac, *The Principles of Quantum Mechanics* (Oxford University Press, Oxford, 1947).

¹³D. M. Brink and G. R. Satchler, *Angular Momentum*, 3rd ed. (Oxford University Press, Oxford, 1993).

¹⁴C. M. M. Nex, M.Sc. dissertation, 1979.

¹⁵We used the real-symmetric diagonalization routine DSYVEX of the LAPACK package.

¹⁶A. Halkier, T. Helgaker, P. Jørgensen, W. Klopper, H. Koch, J. Olsen, and A.K. Wilson, Chem. Phys. Lett. **286**, 243 (1998).

¹⁷J.P. Perdew and A. Zunger, Phys. Rev. B **23**, 5048 (1981).

¹⁸C. Lee, W. Yang, and R.G. Parr, Phys. Rev. B **37**, 785 (1988).

¹⁹J.P. Perdew and Y. Wang, Phys. Rev. B **45**, 13 244 (1992).

²⁰J.P. Perdew, K. Burke, and M. Erzenhofer, Phys. Rev. Lett. **77**, 3865 (1996).

²¹R. D. Amos, Tech. Rep., University of Cambridge, 1995, a suite of quantum chemistry programs developed by R. D. Amos with contributions from I. L. Alberts, J. S. Andrews, S. M. Colwell, N. C. Handy, D. Jayatilaka, P. J. Knowles, R. Kobayashi, K. E. Laidig, G. Lamming, A. M. Lee, P. E. Maslen, C. W. Murray, J. E. Rice, E. D. Simandiras, A. J. Stone, M. D. Su and D. J. Tozer.

²²R. Colle and D. Salvetti, Theor. Chim. Acta **37**, 329 (1975).

²³C.J. Umrigar and X. Gonze, Phys. Rev. A **50**, 3827 (1994).